Steel and Composite Structures, *Vol. 18, No. 1 (2015) 135-148*
DOI: http://dx.doi.org/10.12989/scs.2015.18.1.135

Research on rib-to-diaphragm welded connection by means of hot spot stress approach

Binhua Wang *, Pengmin Lu and Yuhong Shao

Mailbox 312, Chang'an University, The middle section of nan erhuan road, Xi'an City, Shaanxi Province 710064, P.R. China

(*Received March 15, 2013, Revised April 30, 2014, Accepted May 03, 2014*)

Abstract. The cutout hole locating at the place of rib-to-diaphragm welded connection is adopted to minimize the restraint, which is caused by the floor-beam web to rib rotation at the support due to the unsymmetrical loads in orthotropic deck. In practice, an inevitable problem is that there is a large number of welding joint's cracks formed at the edge of cutout hole. In this study, a comparative experiment is carried out with two types of cutout hole, the circular arc transition and the vertical transition. The fatigue life estimation of specimens is investigated with the application of the structural hot spot stress approach by finite element analyses. The results are compared with the ones of the fatigue tests which are carried out on these full-scale specimens. Factors affecting the stress range are also studied.

Keywords: finite elements; orthotropic deck; rib-to-diaphragm welded connection; fatigue; hot spot stress

1. Introduction

Because of its light weight and good economy, orthotropic steel decks, which are fabricated with longitudinal ribs, diaphragm plates and floorings, have been widely applied in the design of long-span steel bridges and also in deck replacement of existing bridges in many parts of the world (Robert 2004). Michèle *et al*. (2005) presented that the concentrated loads by vehicles have great influence on lots of welded structures. For now, lots of early fatigue cracks of welded structures have been reported in similar bridges (Backer *et al*. 2008, Aygül *et al*. 2012, Kolstein 2007, Miki and Tateishi 1997, Xiao *et al*. 2008). In order to minimize the restraint caused by the floor-beam web to rib rotation at the support due to unsymmetrical loads, one often designs a cutout hole to avoid the high stress at the bottom portion of the rib. However, in practical engineering, a large number of welding joint's cracks are formed at the edge of cutout holes (Choi and Kim 2008). The cracks are generated under the two kinds of stress conditions. One is the wheel load located at the top of diaphragm, the other is the wheel load located between diaphragms. These two kinds of stress amplitudes are shown in Fig. 1. Wolchuk and Ostapenko (1992) showed that the out-of-plane moment stress caused by stress status; ① is the main reason of causing cracks between longitudinal ribs and diaphragm plates. The code of AASHTO also details the classification of

*Corresponding author, Ph.D., E-mail: wangbh@chd.edu.cn

http://www.techno-press.org/?journal=scs&subpage=8 ISSN: 1229-9367 (Print), 1598-6233 (Online)

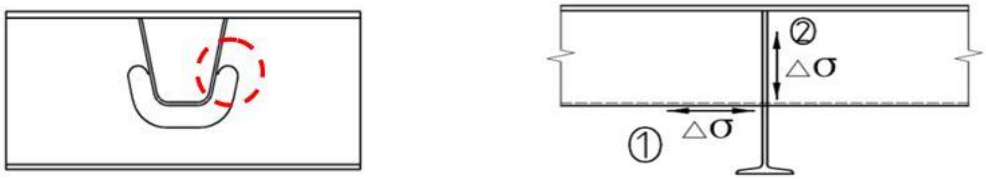

(a) (b)

Fig. 1 Stress state between longitudinal rib and diaphragm plate

stress status ①. But it is not clear for stress status ②. Therefore, for the sake of reducing the stress amplitudes and increasing the fatigue strength of this structure, it is important and crucial to design the reasonable detail structure.

Generally, the fatigue design and analysis of steel bridge are carried out by means of the nominal stress approach. There are several S-N curves with the corresponding fatigue classifications provided for a number of steel details in various codes. And this approach is applied

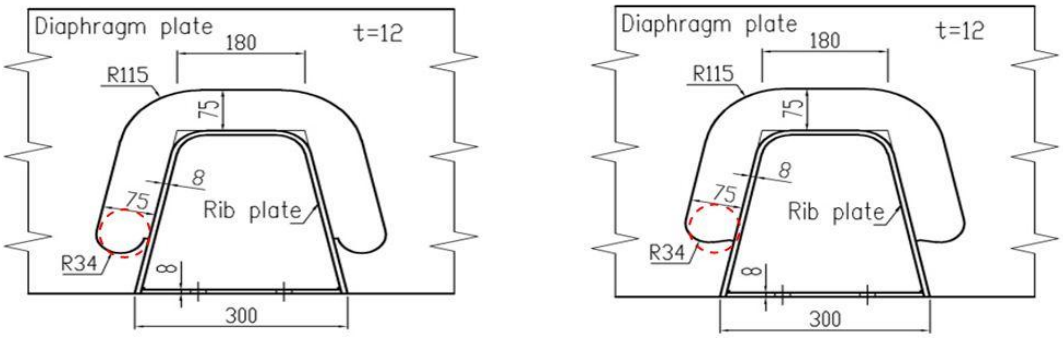

(a) s1:circular arc transition (b) s2: vertical transition

Fig. 2 Sketch of specimens (Unit: mm)

(a) s1:circular arc transition (b) s2: vertical transition

Fig. 3 Photo of specimens

Table 1 The chemical composition and mechanical properties of Q345qD

Category	The chemical composition					The mechanical properties	
	C% Max	Si% Max	Mn%	P% Max	S% Max	Yield strength / MPa	Tensile strength / MPa
Q345qD	0. 18	0.60	1.1-1.6	0.025	0.025	305-345	490-510

according to the average stress in the section of interest, assuming elastic material behavior and ignoring the local stress concentration effects of the weld feature. Due to the complexity in geometry and load transfer conditions between longitudinal ribs and diaphragm plates, it is difficult to estimate the cross-section nominal stress. With the rapid development of computer technology, the hot spot stress approach based on finite element analysis has provided a more convenient and reliable method of design (Aygül *et al*. 2013). The hot spot stress approach also can be used for the structures with the more complex shapes and load statuses in various engineering fields. However, much less attention has been paid on applying hot spot stress approach in orthotropic steel decks. The steel details are always updated constantly in advance of the revision of design specifications. For these reasons, the research on fatigue strength assessment of welded details by utilizing hot spot stress approach has great significance for the engineering.

In this paper, two kinds of rib-to-diaphragm fatigue specimens, which have two different kinds of cutout holes, are designed according to the stress status consistent with actual detail. The specimens are shown in Figs. 2 and 3. Specimen 1, or s1 for short, has the form of circular arc transition as shown in Fig. 2(a); specimen 2, or s2 for short, has the form of vertical transition as shown in Fig. 2(b). The diaphragm thickness is 12mm and the rib thickness is 8 mm. The type of steel is Q345qD. The mechanical properties and chemical composition are shown in Table 1. The hot spot stress methods with several kinds of finite element models are applied to these details. In addition, the structural hot spot stresses evaluated experimentally are compared with simulation results.

2. Fatigue test

The structural hot spot stress cannot be obtained directly from the finite element results. Generally, the linear or quadratic surface stress extrapolation technique is applied to determine the structural hot spot stresses. The International Institute of Welding (IIW) recommendations for ‘type a’ hot spot points are followed when applying the linear stress extrapolation introduced by Hobbacher (2008) in Fig. 4. Accordingly, the two strain gauges (Guage1 and Guage 2) with the length of 1 mm are laid along the direction perpendicular to the weld toe in Fig. 5. The distances from the weld toe are 0.4 t and 1.0 t (rib thickness t), respectively. Each specimen is firstly loaded statically with a load well below that corresponding to yielding to measure the strain distribution at predetermined locations.

Constant amplitude fatigue tests are carried out at the five different load levels, followed by the group test executed at the middle load level. In most cases, the length of cracks that are detected is 20-30 mm, which has been defined as the failure criterion for the fatigue life evaluation in this study. In order to obtain accurate date, the cameras with a macro mode and the scale papers are placed beside the weld toe.

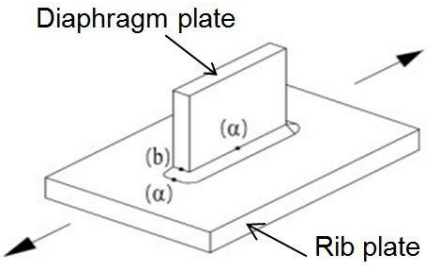

Fig. 4 Hot spot stress types

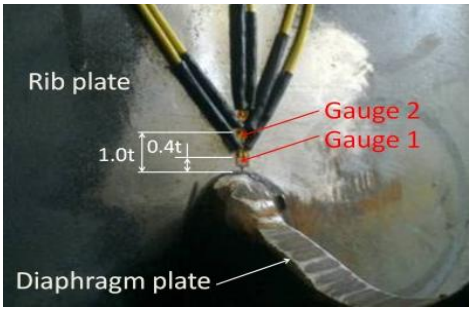

Fig. 5 Arrangement diagram of strain gauges

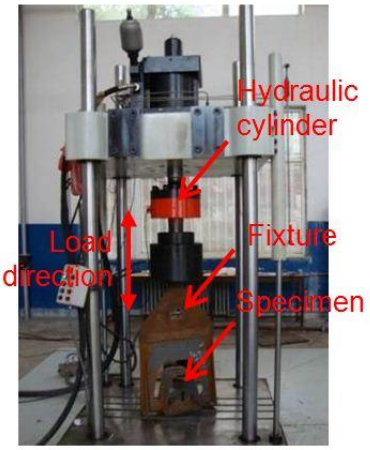

(a) Full-scale specimen

(b) Cameras with a macro mode

Fig. 6 Photos of fatigue test

Table 2 Fatigue test results

Specimen	Num	Frequency /Hz	ΔF /kN	Number of cycles
s1	s1-1	2	120	1409107
	s1-4	2	150	736535
	s1-9	2	180	331072
	s1-3	2	180	1059280
	s1-5	2	180	435607
	s1-10	2	180	205567
	s1-12	2	180	241068
	s1-16	2	200	409925
	s1-13	2	270	82632
s2	s2-1	2	180	1476072
	s2-2	2	180	1085880
	s2-3	2	180	518140

Fig. 7 Fatigue crack in s1

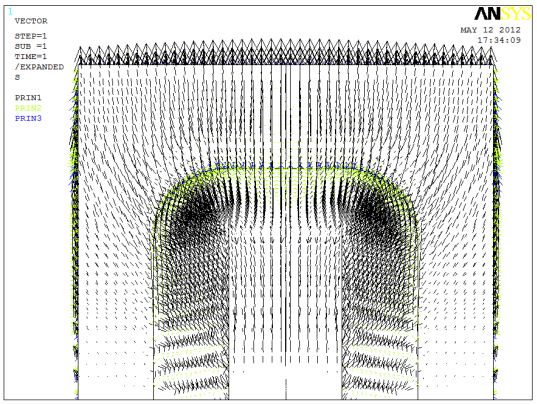

Fig. 8 Principle stress distribution in s1

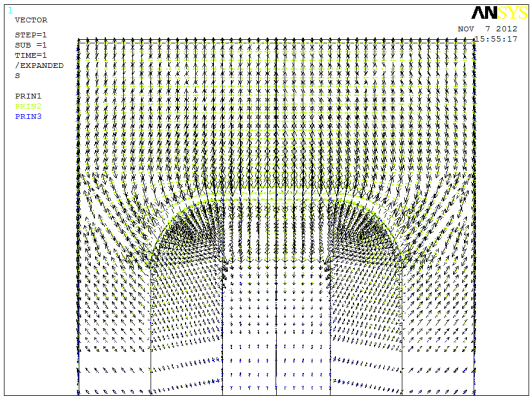

Fig. 9 Principle stress distribution in s2

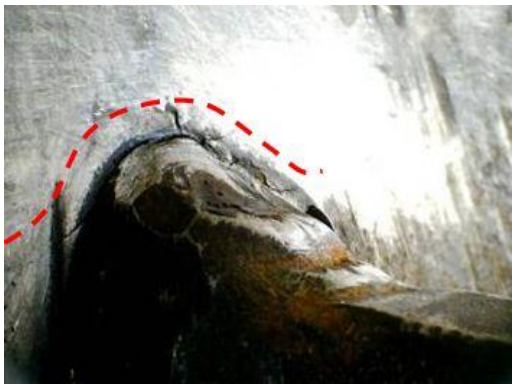

Fig. 10 Fatigue crack in s2

The interval time of taking photo automatically is 30 minutes. The photos of test are shown in Fig. 6 and the result of fatigue tests are shown in Table 2.

There are 9 valid test results among 13 fatigue tests of s1. In all tested specimens, the fatigue cracks firstly starts at the weld toe in the web plate of rib and then propagates along the direction perpendicular to diaphragm plates, as shown in Fig. 7. Compared with the 1st principle stress distribution obtained by finite element analysis, the cracks are propagated along the direction perpendicular to 1st principle stress, as shown in Fig. 8. There are 3 fatigue tests of s2 carried on at the 180 kN of load amplitude and the distribution of 1st principle stress is shown in Fig. 9. Test results are shown in Table 2 and Fig. 10. The cracks of s1 and s2 have the similar crack shapes.

3. Finite element analysis

The element type and mesh size have great effect on the results of finite element model. The result of finite element analysis is highly mesh sensitive. In this study, in order to guarantee the feasibility and accuracy of the fatigue life assessment methods using the finite element methods

for orthotropic bridge deck details, especially the structural hot spot stress approach, we establish several various finite element models with different element types and sizes according to IIW recommendations and references. Since the finite element modeling techniques are similar for s1 and s2, only the s1 models are presented in this paper.

3.1 Structural hot spot stress approach

With the purpose of obtaining more accurate hot spot stresses at the weld toe, a finite element model with 20-node solid element is set up. The element size in this region around the hot spot points are set at 1 × 1 × 1 mm^3. However, Aygül *et al*. (2012) considered that the fine mesh must take more computer resources and cut down on the calculation efficiency. Kim *et al*. (2009) promoted different modeling techniques and procedures with shell elements to obtain reliable stress values at fatigue-critical points. Because the investigated crack initiation points are classified as "type a" hot spot points, which is recommended in IIW recommendations, the structural hot spot stresses are calculated by means of linear surface stress extrapolation.

3.1.1 Solid model

Because the double-sided fillet weld is adopted to connect the diaphragm plate with rib web plate, there is a non-connection region between two welding lines in Fig. 11. The contact elements

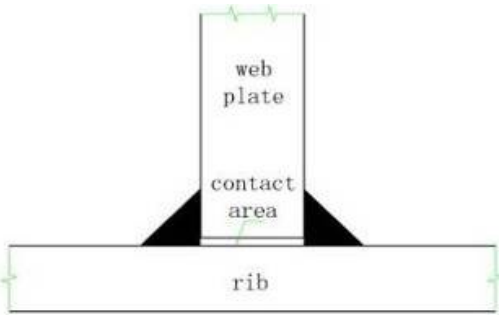

Fig. 11 Sketch of rib-to-diaphragm welded connection

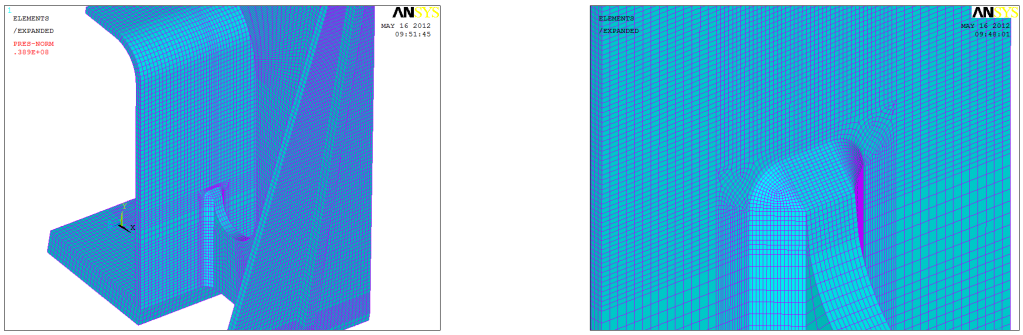

(a) Whole model (b) Submodel

Fig. 12 Solid model

are utilized in this region in Solid Contact model, and the Solid Non-contact model is set up by using the glue technology of software to simulate this region. The technology of submodel is reused in these two models in order to keep the element size around the hot spot points at 1 × 1 × 1 mm^3. Fig. 12 shows the two kinds of solid element models with 20-node solid element.

3.1.2 Shell non weld model and shell weld end model

Two finite element models with 8-node shell element are set up at the place of the middle plates. One model does not contain welding structure and the other one includes it, as shown in Figs. 13 and 14. Fricke (2002) introduced that the distance of stress extrapolation point can be determined starting from the place of rib-to-diaphragm connection when the mesh size is 0.5 t.

3.1.3 Shell inclined weld model

Shell Inclined Weld model with 8-node shell element is set up at the place of the middle plates, as shown in Fig. 15. Some inclined shell elements are used to simulate weld structures. The line ‘ae’ and line ‘ah’ represent the place of shell elements for simulating welding lines and the shell elements are the same thickness as welding throat. Fricke (2002) recommended that the mesh size is 0.5 t and the distance of stress extrapolation point can be determined starting from the place of point h.

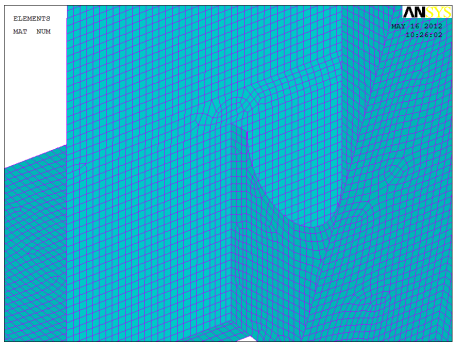

Fig. 13 Shell non weld model

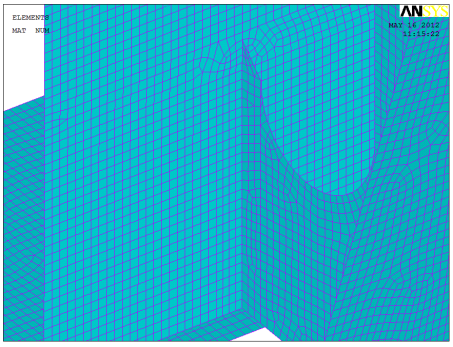

Fig. 14 Shell weld end model

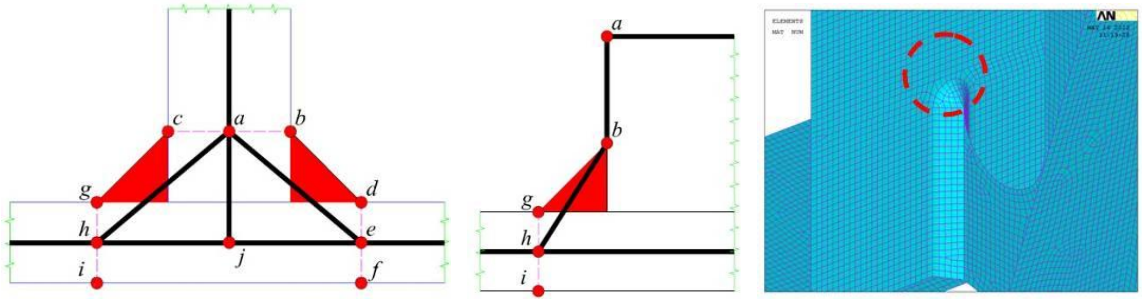

(a) Transverse section of weld model (b) Lateral view of weld toe (c) Finite element model

Fig. 15 Shell inclined model

3.1.4 Shell increased thickness model

According to the reference (Aygül *et al*. 2012), the Shell Increased Thickness model is set up. In order to simulate the affection of welding structure, the shell elements with various thickness parameters are adopted. The thickness of welding region in diaphragm plate is the sum of diaphragm thickness t1 and fillet welding height h. And the thickness of welding region in web plate of rib is the sum of rib thickness t2 and fillet welding height h. The model is shown in Fig. 16.

3.1.5 Shell constraint equation model

According to the reference (Fayard *et al*. 2007), the Shell Constraint Equation model is set up. In order to simplify model, the constraint equations are utilized to simulate the connection between rib web plate and diaphragm plate rather than the rigid elements used by Fayard *et al*. (2007), as shown in Fig. 17.

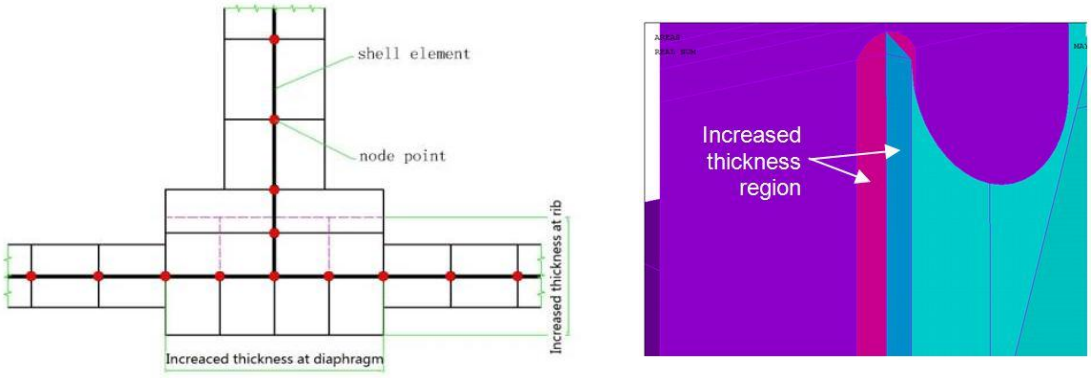

(a) Shell element model (b) Increased thickness region

*t1—diaphragm thickness; t2—rib thickness; h—fillet welding height

Fig. 16 Shell increased thickness model

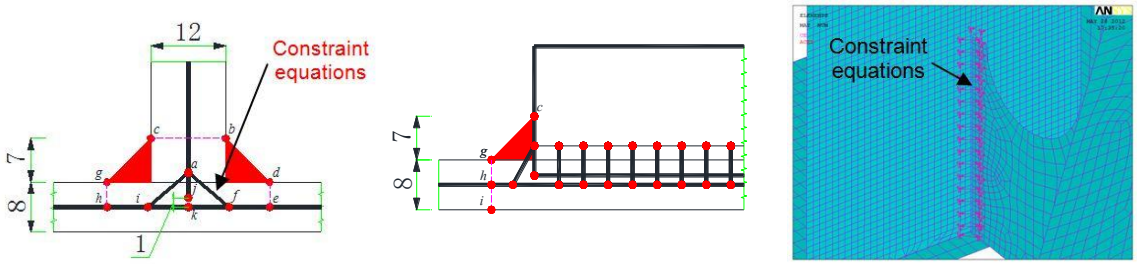

(a) Transverse section of weld model (b) Lateral view of weld toe (c) Constraint equations region

Fig. 17 Shell constraint equation model (Unit: mm)

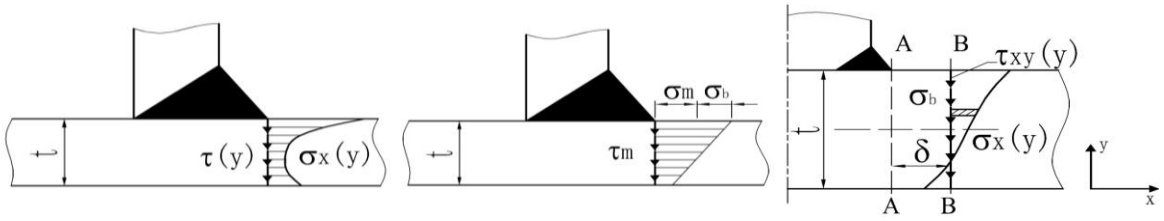

(a) (b) (c)

Fig. 18 Dong's structure stress calculation

3.1.6 Dong's method

The mesh size and element type of the models mentioned above have great effect on the finite element analysis. So Dong (2001) has promoted the way of gaining hot spot stress to avoid the disadvantages of finite element methods according to statically equivalent structural stress distribution, which can be obtained by the solid finite element analysis, as shown in Fig. 18. The nominal stress σ_s of section A-A is composed of membrane stress σ_m and bending stress σ_b

$$\sigma_s = \sigma_m + \sigma_b \tag{1}$$

A second reference plane can be defined along Section B–B in Fig. 18(c). By imposing equilibrium conditions between Sections A–A and B–B, the structural stress components σ_m and σ_b must satisfy the following conditions

$$\sigma_m = \frac{1}{t}\int_0^t \sigma_x(y)\cdot dy \tag{2}$$

$$\sigma_m \cdot \frac{t^2}{2} + \sigma_b \cdot \frac{t^2}{6} = \int_0^t \sigma_x(y)\cdot y \cdot dy + \delta\int_0^t \tau_{xy}(y)\cdot dy \tag{3}$$

3.2 Evaluation of structural hot spot stresses of s1

In order to enable a comparison between the measured and calculated hot spot stresses at the weld toe, the hot spot stresses from the 7 different finite element analyses and from the static tests are calculated at the same points where the strain gauges are placed at the load of 120 kN. This comparison is also used as a means of verifying the finite element model. Evaluation results of s1 are shown in Fig. 19. The calculated hot spot stresses of 7 different finite element models at 0.4 t distance from the weld toe have greater diversity than those at 1.0 t distance from the weld toe. The result indicates that the diverse modeling methods have great influence on the stress distribution at weld toe region. Compared with the measured results, the solid element models, both using contact elements and non-contact elements, present a good estimation of the hot spot stresses. In order to simplify the model, the solid element model with non-contact elements is recommended. So the solid element model of s2 is set up only by using non-contact elements. The Shell Weld End model and the shell model with constraint equations representing the welds also yield good results when compared with the other shell element models included in the model. The

result gained through the Shell Increased Thickness model cannot yield good agreement with the test results. So the Shell Increased Thickness model is not presented here. The Dong's method proposed by Dong yields good results for investigated point because this calculated stress is obtained based on the stress distribution by means of the solid element model.

Besides, the fatigue life of the s1 is estimated in terms of the structural hot spot stress approach. Then the results are plotted by means of linear regression analysis on the base of the results of solid model with a slope of 3 to compare with the fatigue design class C90, C100 and C112 according to EC3, as shown in Fig. 20. The two S-N curves, i.e., FAT90 and FAT100, are also recommended for the structural hot spot stress approach in IIW.

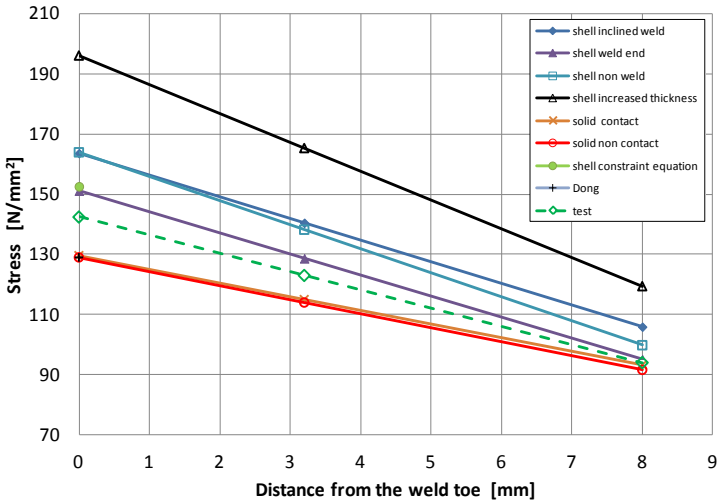

Fig. 19 Evaluation results of s1 at the load of 120 kN

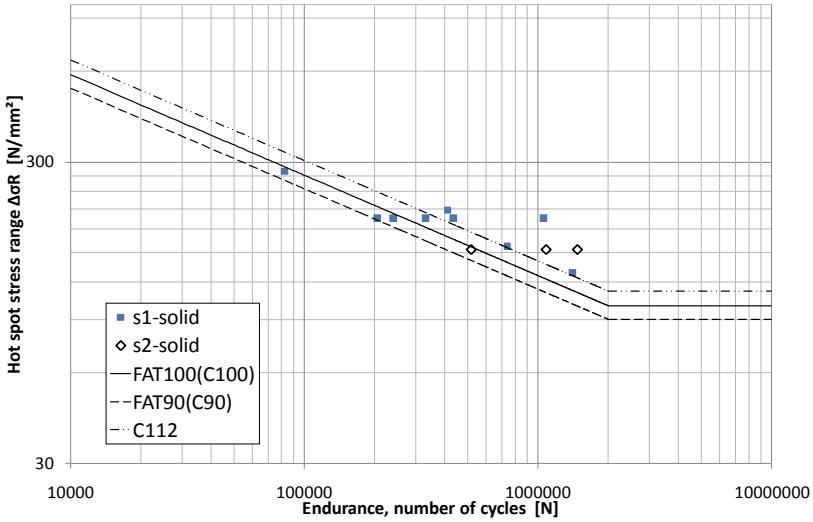

Fig. 20 Fatigue test results by means of the structural hot spot stress

3.3 Evaluation of structural hot spot stresses of s2

For the s2, the hot spot stresses from 6 different finite element models (excluding solid contact model) and from the static tests are also calculated at the same points where the strain gauges are placed at the load of 120 kN. Evaluation results of s2 are shown in Fig. 21. Compared with the measured results, the solid element models using non-contact elements, the Dong's method, the Shell Weld End element model and the shell model with constraint equations present a good estimation of the hot spot stresses. Compared with the hot spot stress of s1, the hot spot stress of s2 that are calculated by means of various methods are lower, as shown in Table 3. The hot spot stress of s2 has at least exceeded those of s1 by nearly 21 percent.

In addition, the fatigue life of the s2 is estimated in terms of the structural hot spot stress approach. Then the results are plotted by means of linear regression analysis on the base of fatigue

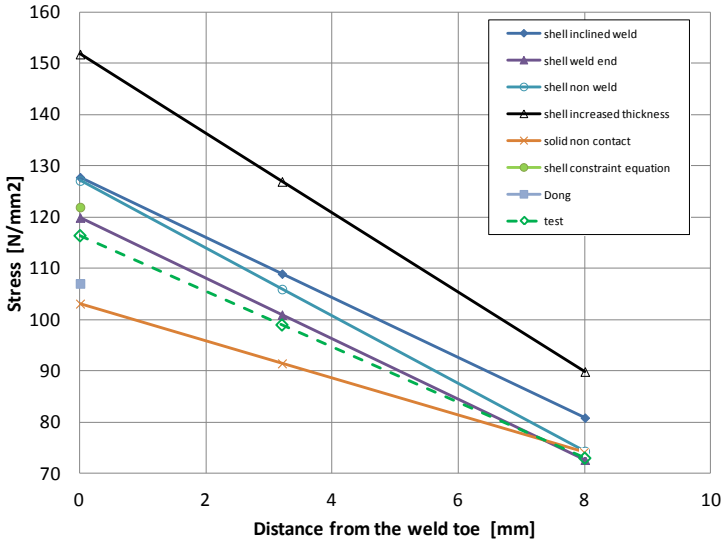

Fig. 21 Evaluation results of s2 at the load of 120 kN

Table 3 The table comparing the hot spot stress of s1 with the hot spot stress of s2 at the load of 120 kN

Analysis model	s1 /MPa	s2 /MPa	$\frac{\sigma_{hs1}-\sigma_{hs2}}{\sigma_{hs2}}$
shell inclined weld	164	128	28%
shell weld end	151	120	26%
shell non weld	164	127	29%
shell increased thickness	196	152	29%
solid non contact	129	103	25%
shell constraint equation	153	122	25%
Dong	129	107	21%
test	142	116	22%

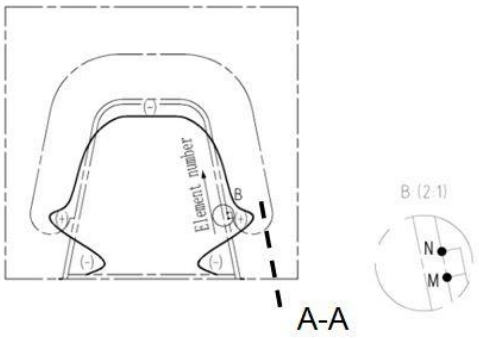

Fig. 22 Rib bending moment distribution

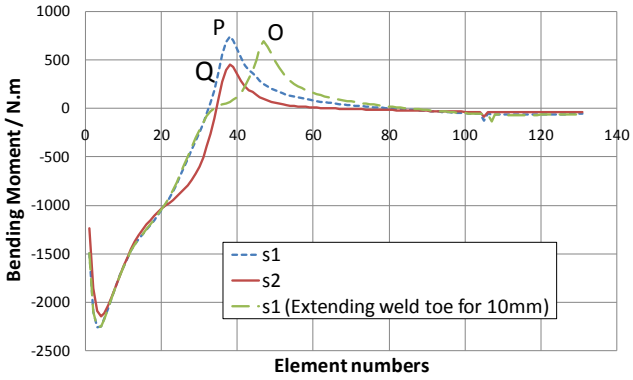

Fig. 23 The bending moment distribution of s1 and s2

test at the load of 180 kN, with a slope of 3 to compare with the recommend fatigue design class C90, C100 and C112 according to EC3, as shown in Fig. 20. As we can see from the result, the s2 with the vertical transition structure has the higher fatigue strength than the s1 with the circular arc transition structure.

3.4 Analyzing reasons

During the structural design, the circular arc transition structure is always used to decrease the concentrated stress. However, the s1 with circular arc transition structure has higher hot spot stress at weld toe region than the s2 with vertical transition structure. The reasons are as follows. The height of s1 is lower than that that of specimen 2 at A-A section. So the bending elastic modulus of s1 is smaller than that of s2. And then the stress induced by bending moment at s1 is higher than it at s2. The bending moment at rib is shown in Fig. 22. And the bending moment of s1 and s2 calculated by Shell Weld End model is shown in Fig. 23. The bending moment at weld toe region, such as point *P* and point *Q*, are shown. The bending moment of point *P* is higher than that of point *Q*. It can be concluded that the effect of decreasing concentrated stress using the circular arc transition structure of s1 is less than that of decreasing concentrated stress using the vertical transition structure of s2. In addition, in order to reduce the hot spot stress of s1 at weld toe region, the Shell Weld End model by extending point *M* to point *N* for 10 mm is set up, as is shown in Fig. 22, and the rib bending moment is shown in Fig. 23. Apparently the new weld toe region, such as point *O*, has a lower moment than point *P*, but the bending moment at point *O* is significantly higher than that at point *Q*. The fact indicates that the s2 has the apparent ability to cut down the hot spot stress at weld toe region.

4. Conclusions

Fatigue assessment of a rib-to-diaphragm welded connection considering two structure styles with the circular arc transition structure and the vertical transition structure is carried out by using hot spot stress approach and full-scale fatigue tests. Based on the results, the main findings of this study are as follows:

- The calculated hot spot stresses of 7 different FE analyses at 0.4 t distance from the weld toe have greater diversity than those at 1.0 t distance from the weld toe. The results show that the diverse modeling methods have great influence on the stress distribution at weld toe region.
- Compared with the measured results, the solid element models, both using contact elements and non-contact elements, present a good estimation of the hot spot stresses. Therefore, in order to simplify the model, the solid element model with non-contact elements is recommended.
- The Shell Weld End element model and the shell model with constraint equations representing the welds also yield good results when compared with the other shell element models included in the model. However, the result that is gained through the shell increased thickness model cannot yield good agreement with the test result and this model is therefore not presented for these details.
- The Dong's method proposed by Dong can gain good results for investigated point because this calculated stress is obtained based on the stress distribution by means of the solid FEA.
- Compared with the hot spot stress of s1, the hot spot stress of s2 has at least exceeded that of s1 by nearly 21 percent at the load of 120 kN, And according to the fatigue test results by means of the structural hot spot stress, the fatigue life of the s2 is higher than that of s1.
- Through the analysis of bending moment, it can be concluded that the effect of decreasing concentrated stress using the circular arc transition structure at s1 is less than that of decreasing concentrated stress using the vertical transition structure at s2. So the structure of s2 with higher fatigue life is presented at the rib-to-diaphragm welded connection.

Acknowledgments

This work is supported by the research fund of the communication department of Jiangxi province (2010C00003), the funding of China Scholarship Council (201306565024) and the Fundamental Research Funds for the Central Universities (2013G1251032).

References

Aygül, M., Al-Emrani, M. and Urushadze, S. (2012), "Modelling and fatigue life assessment of orthotropic bridge deck details using FEM", *Int. J. Fatigue*, **40**, 129-142.

Aygül, M., and Bokesjö, M., Heshmati, M. and Al-Emrani, M. (2013), "A comparative study of different fatigue failure assessments of welded bridge details" *Int. J. Fatigue*, **49**, 62-72.

Backer, H.D., Outtier, A. and Van Bogaert, P. (2008), "Analytical calculation of internal forces in orthotropic plated bridge decks based on the slope-deflection method", *J. Construct. Steel Res.*, **64**(12), 1530-1539.

Choi, J.H. and Kim, D.H. (2008), "Stress characteristics and fatigue crack behaviour of the longitudinal rib-to-Cross beam joints in an orthotropic steel deck", *Adv. Struct. Eng.*, **11**(2), 189-198.

Dong, P. (2001), "A structural stress definition and numerical implementation for fatigue analysis of welded joints", *Int. J. Fatigue*, **23**(10), 865-876.

Fayard, J.L., Bignonnet, A. and Dang Van, K. (2007), "Fatigue design criterion for welded structures", *Fatigue Fracture Eng. Mater. Struct.*, **19**(6), 723-729.

Fricke, W. (2002), "Recommended hot-spot analysis procedure for structural details of ships and FPSOs based on Round-Robin FE analyses", *Int. J. Offshore Polar Eng.*, **12**(1), 89-96.

Hobbacher, A. (2008), "Recommendations for fatigue design of welded joints and components", IIW Doc. IIW-1823-07.

Kim, M.H., Kim, S.M., Kim, Y.N., Kim, S.G., Lee, K.E. and Kim, G.R. (2009), "A comparative study for the fatigue assessment of a ship structure by use of hot spot stress and structural stress approaches", *Ocean Eng*., **36**(14), 1067-1072.

Kolstein, K.H. (2007), "Fatigue classification of welded joints in orthotropic steel bridge decks", Ph.D. Dissertation, Delft University of Technology, The Netherlands.

Michèle, S.P., Battista, R.C. and Mergulhão, A.J.R. (2005), "Stress concentration in steel bridge orthotropic decks", *J. Construct. Steel Res*., **61**(8), 1172-1184.

Miki, C. and Tateishi, K. (1997), "Fatigue strength of cope hole details in steel bridges", *Int. J. Fatigue*, **19**(6), 445-455.

Robert, J.C. (2004), "Influence of cutout geometry on stresses at welded rib-to-diaphragm connections in steel orthotropic bridge decks", *J. Transport. Res. Board*, **1892**, 78-87.

Wolchuk, R. and Ostapenko, A. (1992), "Secondary stresses in closed orthotropic deck ribs at floor beams", *J. Struct. Eng*., **118**(2), 582-595.

Xiao, Z.G., Yamada, K., Ya, S. and Zhao, X.L. (2008), "Stress analyses and fatigue evaluation of rib-to-deck joints in steel orthotropic decks", *Int. J. Fatigue*, **30**(8), 1387-1397.

CC